

Article

# The Potential of Membrane Contactors in the Pre-Treatment and Post-Treatment Lines of a Reverse Osmosis Desalination Plant

Alessandra Criscuoli 

Institute on Membrane Technology (CNR-ITM), via P. Bucci 17/C, 87036 Rende, Italy; a.criscuoli@itm.cnr.it; Tel.: +39-0984-492118

**Abstract:** The flexibility of membrane contactors (MCs) is highlighted for a reverse osmosis (RO) desalination plant. MCs are applied as pre-treatment for the oxygen removal and the pH reduction of seawater, also as post-treatment for the pH increase of the RO permeate and the reduction of the RO brine volume. A decrease of the seawater pH down to neutral values, as needed when coagulation is used in the pre-treatment line of RO, together with an increase of the RO permeate pH up to 7.58, matching the target of produced water, can be obtained without the use of chemicals. Direct Contact Membrane Distillation (DCMD) and Vacuum Membrane Distillation (VMD) are investigated as function of the feed concentration (ranging from 40 g/L to 80 g/L) and temperature (40 °C–80° C). Their performance is compared at parity of operating conditions and in terms of applied driving force. Both distillation systems are able to efficiently reject salts (rejection > 99.99%), while higher distillate fluxes are obtained when a vacuum is applied at the permeate side (15 kg/m<sup>2</sup>h vs. 6.6 kg/m<sup>2</sup>h for the 80 g/L feed).

**Keywords:** membrane contactors; RO desalination plants; pre- and post-treatments; RO brine reduction



**Citation:** Criscuoli, A. The Potential of Membrane Contactors in the Pre-Treatment and Post-Treatment Lines of a Reverse Osmosis Desalination Plant. *Separations* **2023**, *10*, 129. <https://doi.org/10.3390/separations10020129>

Academic Editors: Mingheng Li and Zhenghua Zhang

Received: 13 December 2022

Revised: 6 February 2023

Accepted: 9 February 2023

Published: 14 February 2023



**Copyright:** © 2023 by the author. Licensee MDPI, Basel, Switzerland. This article is an open access article distributed under the terms and conditions of the Creative Commons Attribution (CC BY) license (<https://creativecommons.org/licenses/by/4.0/>).

## 1. Introduction

Desalination is today one of the major sources of fresh water, a response to the water scarcity which afflicts the planet. Plants based on reverse osmosis (RO) are quickly replacing thermal plants, due to the lower energy consumption. In RO, the semipermeable membrane is able to be permeated at ambient temperature mostly by water, while the dissolved species are blocked at the retentate side. Starting from seawater, two streams are then produced: the permeate fresh water, which is depleted of most of the elements (including monovalent ions); and the rejected brine, which is concentrated in the elements contained in the seawater. Because of the osmotic limitations, water-recovery factors not exceeding 50% can be obtained. Both pre-treatments and post-treatments are required in RO plants. Pre-treatments are needed to reduce fouling issues in RO modules, as well as to control the oxygen content and the pH of the seawater. In particular, the oxygen content has to be controlled to avoid problems of corrosion, oxidation processes, and biogrowth. Also, the pH must be adjusted to match the requirements of the pre-treatment methods employed, as well as those of the RO membrane, and to control the precipitation of species, which could lead to scaling problems in the plant. Similarly, during post-treatments, in addition to the remineralization of the permeate, the pH of the product water must be at the target value [1]. The oxygen removal is usually carried out in vacuum towers, eventually coupled with oxygen scavengers, while the pH control is often obtained by adding acids (e.g., H<sub>2</sub>SO<sub>4</sub> is often employed when coagulation is used as RO pre-treatment) and bases (e.g., NaOH). Sometimes the pH increase is also obtained by CO<sub>2</sub> stripping. Concerning the brine produced, no specific treatments are employed, as it is discharged back to the sea, injected into deep wells, sent into sewers, or collected in solar ponds. However, these common practices cause serious impacts on the environment and disturbance of the marine ecosystem [2–5]. Figure 1 shows the conventional pre- and post- treatments used to control the pH and the oxygen content in an RO desalination plant.

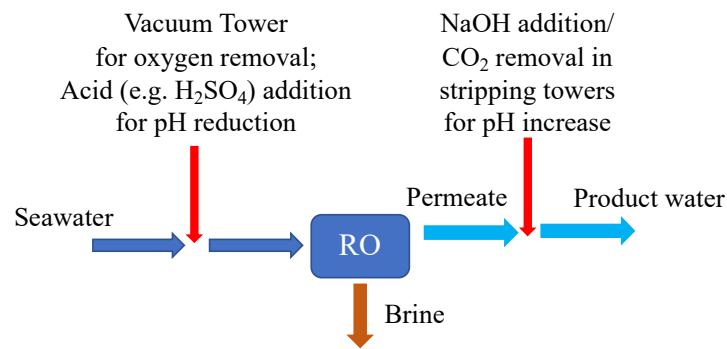


**Figure 1.** Conventional pre- and post-treatments used for oxygen and pH control in an RO desalination plant.

Since their first appearance, dating back to early 1990s, membrane contactors have been applied in different fields, including the carbonation of beverages, treatment of boiler feedwater (deoxygenation), ultrapure water production for the semiconductor industry, blood oxygenators, extraction of acidic gases from flue gases, extraction of metals from contaminated wastewaters, etc. [6,7]. In MCs, microporous membranes are not used for their selective properties, but for providing an interface between phases. Once the phases are in contact at the micropore mouth, the species can move from one phase to the other by diffusion, with the driving force being the difference in concentration. MCs are characterized by a high interfacial area, which leads to very compact devices. When compared with vacuum towers for the oxygen removal from seawater, MCs working with a combination of stripping gas and vacuum (combo mode) show a higher removal efficiency, a lower weight and a smaller footprint, a lower cost for maintenance (chemicals are not required), and a greater modularity [8–10]. Membrane distillation (MD) is another membrane operation belonging to the MCs family. Microporous hydrophobic membranes are used to evaporate a hot feed (typically from 40 °C to 80 °C), preventing the passage of water as liquid. Therefore, at the permeate side, a high-purity water (distillate) is collected, while all non-volatile species are concentrated on the feed side. The driving force is a difference in vapor pressure across the membrane, which can be obtained in different ways, depending on the MD configuration. In the Direct Contact Membrane Distillation, a cold stream (distillate), in which the vapor condenses, is sent at the other side of the membrane, while in Vacuum Membrane Distillation, the permeate is kept under vacuum and the vapor condenses outside the MD module. Figure 2 shows the vapor removal from the hot feed through the membrane micropore, for the two MD configurations.

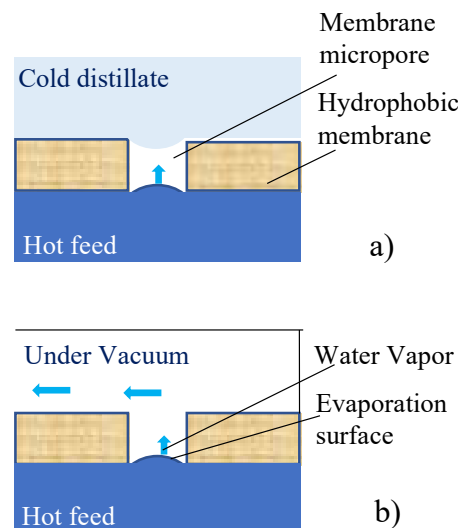


**Figure 2.** (a) DCMD and (b) VMD configurations.

With respect to RO, MD can also be used with high feed concentrations, being affected to a minor extent by concentration-polarization phenomena while not suffering from osmotic limitations. Based on this feature, different studies have been carried out to further concentrate the RO brine by MD, so as to produce more fresh water and to reduce the brine volume to be disposed. In particular, different MD configurations have been investigated using different modules, membranes and operating conditions [11–22]. Considering the state of the art in the field, MCs could play an interesting role in RO desalination plants. This work is intended to further assess and extend the application of MCs in the pre-treatment and post-treatment lines, highlighting their flexibility, which is an important aspect in the plant design. In a previous study, MCs were experimentally investigated to control both the oxygen removal and the pH in different points of an integrated nanofiltration (NF)-RO desalination plant (NF feed, NF permeate, RO brine and RO permeate), resulting in a possible option to reduce the use of chemicals [23]. Hydrophobic membranes were employed to block the liquid phase at the pore mouth, while allowing the permeation of the gaseous phase inside the pore. The obtained outcomes are now considered in some case studies regarding the seawater pre-treatment and the permeate post-treatment of an RO plant, so as to investigate whether MCs can have a role in reaching the target values of a real RO desalination plant. The pre-treatment considered consists of the use of MCs for the oxygen removal coupled with the pH reduction of seawater (see Figure 3a), while the post-treatment focuses on the pH increase of the produced water (see Figure 3b). To the best of the Author’s knowledge, no other data are available in literature on the application of membrane contactors for the simultaneous control of the oxygen content and pH, as well as for the pH adjustment, in desalination. Furthermore, to highlight the flexibility of MCs, the same module used for the gas-liquid operation is employed to carry out MD tests on the RO brine. In particular, the performance of DCMD and VMD for treating the RO brine are compared in terms of flux and permeate conductivity. The possibility of having a versatile module for different processes makes plant design easier and cheaper. Moreover, the use of the same module, membrane and operating conditions for the RO brine treatment, allows a direct comparison of the MD configurations performance, not often possible when based on literature studies, because of the different modules, membranes, operating conditions and MD configurations investigated. Figure 4 summarizes the main steps followed in this work.

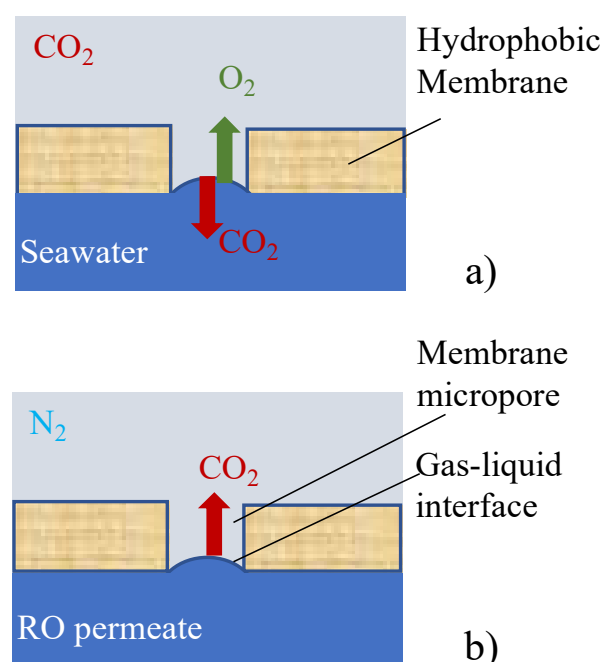


Figure 3. (a) Seawater pre-treatment and (b) RO permeate post-treatment by membrane contactors.

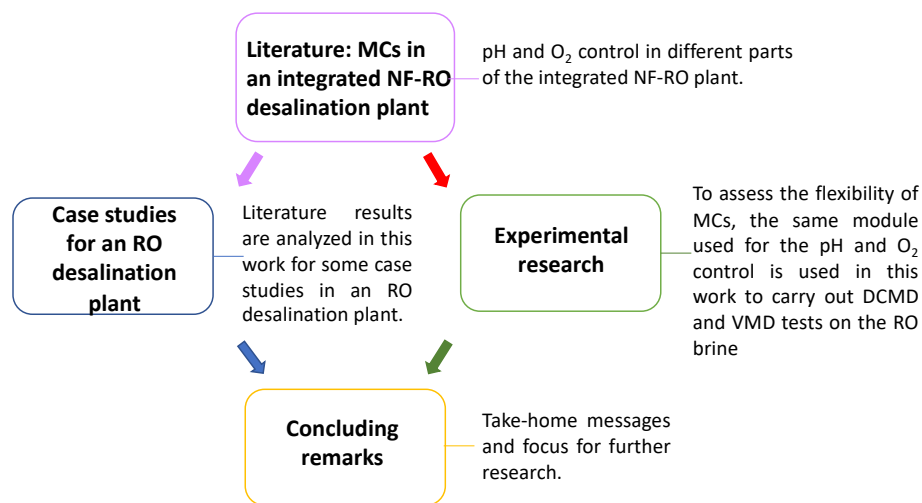


Figure 4. Main steps followed in this work.

## 2. Materials and Methods

The same module was used for the different applications and, depending on the type of treatment, CO<sub>2</sub>, N<sub>2</sub>, cold water, or vacuum were considered for the permeate side.

The module used to carry out the gas-liquid and MD tests had a flat configuration (40 cm<sup>2</sup> membrane area), and was made of two plates in nylon, between which the hydrophobic membrane was located. In both applications, the liquid flow rate was fixed at 200 L/h, being the maximum value at which the set-up operated without an increase in the pressure drop. The corresponding feed velocity was 0.4 m/s (Reynolds (*Re*) values of 2576 at 20 °C, 3680 at 40 °C, and 7360 at 80 °C).

### 2.1. Gas-Liquid Operation

#### 2.1.1. Gas-Liquid Set-Up

The liquid was recirculated at the bottom side of the membrane, while the gas was sent, in continuous mode at the top side. CO<sub>2</sub> and N<sub>2</sub> were used as gaseous streams, for liquid pH reduction and increase, respectively. The oxygen content and the pH of the liquid were measured by a dissolved oxygen meter and a pH meter, respectively. More details of the gas-liquid set-up are reported in [23]. A picture of the set-up is shown in the Supplementary Material (Figure S1).

#### 2.1.2. Theoretical Section: Mass Transfer Resistances Involved in Gas-Liquid Membrane Contactors

When membrane contactors are applied in gas-liquid operations, three resistances are involved in the transport of gaseous species, as depicted in Figure 5: the one offered by the liquid phase, the one of the membrane, and the one of the gas phase.

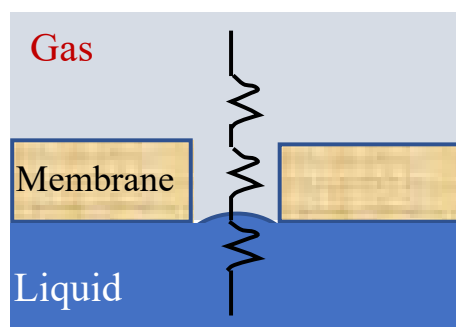


Figure 5. Sketch of mass transfer resistances in gas-liquid membrane contactors.

The gas phase resistance can usually be disregarded [24], and the transport between phases is regulated by the liquid and the membrane resistances, which are calculated as functions of the respective mass-transfer coefficients:

$$\text{Mass resistance} = \frac{1}{\text{Mass transfer coefficient}} \tag{1}$$

In particular, for  $Re > 2000$ , the mass transfer coefficient of the liquid side ( $k_l$ ) can be calculated by the equation [25]:

$$Sh = 0.023 Re^{0.8} Sc^{0.33} \tag{2}$$

with  $Sc$ , the Schmidt number, and  $Sh$ , the Sherwood number given by:

$$Sh = \frac{k_l d_h}{D} \tag{3}$$

with  $d_h$  (m), the hydraulic diameter and  $D$  ( $m^2/s$ ), the diffusivity of the gaseous species in the liquid.

For a flat geometry, the hydraulic diameter can be calculated by:

$$d_h = \frac{4S}{P} \tag{4}$$

with  $S$  ( $m^2$ ), the cross section, and  $P$  (m), the perimeter of the channel in which the liquid flows.

The mass transfer coefficient of the membrane ( $k_m$ ) can be calculated by considering both the molecular and the Knudsen diffusions following the steps reported below [7,26,27]:

$$k_m = \frac{D_{eff} \epsilon}{\delta \tau} \tag{5}$$

with  $D_{eff}$  ( $m^2/s$ ), the effective diffusivity of the gaseous species in the membrane,  $\epsilon$  (/), the membrane porosity,  $\delta$  (m), the membrane thickness, and  $\tau$  (/), the membrane tortuosity.

The membrane tortuosity can be calculated as a function of the membrane porosity by two different expressions, depending on the compactness of the membrane structure [27].

For a more open structure:

$$\tau = \frac{1}{\epsilon} \tag{6}$$

For a more closed structure:

$$\tau = \frac{(2 - \epsilon)^2}{\epsilon} \tag{7}$$

The effective diffusivity can be obtained by:

$$D_{eff} = \frac{1}{\left(\frac{1}{D_m} + \frac{1}{D_K}\right)} \tag{8}$$

where  $D_m$  ( $m^2/s$ ), is the molecular diffusivity, and the  $D_K$  ( $m^2/s$ ) is the Knudsen diffusivity, that can be calculated by:

$$D_K = \frac{2}{3} r_p \sqrt{\frac{8 R T}{\pi M}} \tag{9}$$

with  $r_p$  (m), the membrane pore radius,  $R$  (J/(mol K)), the gas constant,  $T$  (K), the temperature and  $M$  (kg/mol), the molecular weight.

### 2.2. MD Set-Up

The DCMD and VMD tests were carried out by using a commercial (Membrana, 3M, Wuppertal, Germany) polypropylene membrane (0.2 μm pore size, 70% porosity, 91 μm thickness).

Feeds with different salt concentrations were prepared to simulate seawater (40 g/L), low (58.5 g/L) and high-concentrated (80 g/L) RO brines. Salts (Sigma-Aldrich, Merck, Milano, Italy) were dissolved in deionized water, considering the seawater composition used in [23]. Table 1 summarizes the composition of the feeds.

**Table 1.** Composition of the feeds (g/L) used in MD tests.

Salt	Seawater	Low RO Brine	High RO Brine
NaCl	23.27	33.24	46.54
Na <sub>2</sub> SO <sub>4</sub>	3.99	5.71	8.00
MgCl <sub>2</sub> 6H <sub>2</sub> O	11.28	16.11	22.56
KBr	0.095	0.136	0.19
CaCl <sub>2</sub> 2H <sub>2</sub> O	1.47	2.1	2.94
NaHCO <sub>3</sub>	0.1932	0.276	0.3864
KCl	0.6635	0.948	1.327
Na <sub>2</sub> CO <sub>3</sub> H <sub>2</sub> O	0.0072	0.0103	0.0144

In both configurations, the hot liquid stream was recirculated at the bottom side of the membrane, while a cold liquid stream was recirculated in counter-current mode at the top side (DCMD) or a vacuum was applied at the permeate side (VMD). In the first case, the mass of the permeated vapor was weighed using a balance, on which the distillate tank was located. In VMD, the condensed vapor was collected into a trap, then its mass was weighed. Therefore, by simply acting on the permeate line, it was possible to operate with a different MD configuration, keeping the same operating conditions at the feed side (see Figure 6a,b). Pictures of the two MD set-ups are furnished in the Supplementary Material (Figures S2 and S3).

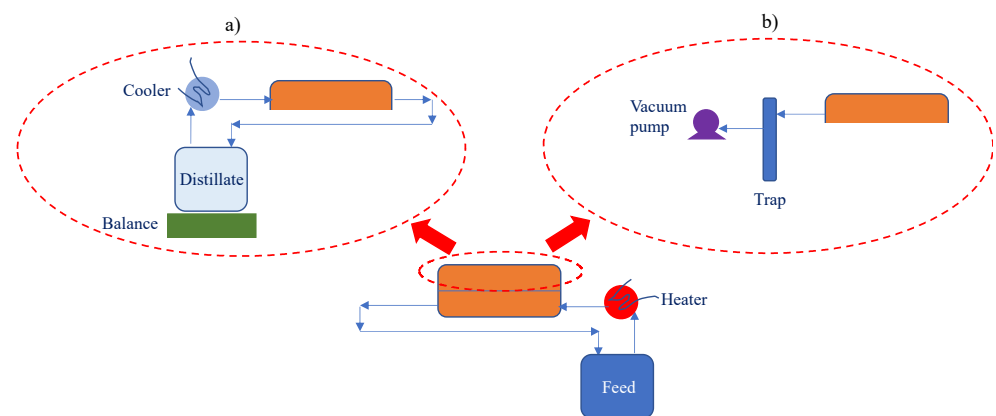


**Figure 6.** (a) DCMD and (b) VMD lab set-ups.

Experiments were carried out at different feed temperatures, by fixing the operating conditions at the permeate side (200 L/h and 18 °C for DCMD, and 20 mbar for VMD). In particular, the operating temperature of the cold stream in DCMD was chosen to work at the permeate side with the same vapor pressure of VMD, meaning the same driving force across the membrane. Each MD test lasted 1 h, to compare the two configurations at the same feed concentration, avoiding a significant change in concentration due to water removal over time. Nevertheless, it has to be noticed that both configurations have been

applied to significantly concentrate the brine, as already reported in the Introduction. For example, the brine was concentrated from 55 g/L to 388 g/L at 75 °C in DCMD, with a flux decrease from 52.3 kg/m<sup>2</sup>h to 17.5 kg/m<sup>2</sup>h [17], and from 64 g/L to 300 g/L at 50 °C in VMD, with a flux decrease from 17 kg/m<sup>2</sup>h to 7 kg/m<sup>2</sup>h [13].

Once the mass of the permeate is known, the permeate flux can be calculated as:

$$J = \frac{m}{A_m \times t} \tag{10}$$

where  $J$  (kg/m<sup>2</sup>h) is the flux,  $m$  (kg) is the permeate mass,  $A_m$  (m<sup>2</sup>) is the membrane area and  $t$  (h) is the experimental time.

The salt rejection is calculated by measuring the conductivity of the feed and of the permeate as follows:

$$R (\%) = \frac{C_f - C_p}{C_f} \tag{11}$$

where  $C_f$  and  $C_p$  are the conductivity (S/m) of the feed and of the permeate, respectively.

Both equations are commonly used to calculate the flux and the rejection in membrane distillation for desalination [11–22].

### 3. Results and Discussion

#### 3.1. Oxygen Removal and pH Control

The results obtained in [23] were applied to two case studies of an RO desalination plant, as reported in the following part.

##### 3.1.1. Case Study 1: The Pre-Treatment of Seawater to Remove Dissolved Oxygen and to Reduce the pH

The oxygen content of seawater has to be reduced before entering the RO desalination plants (target value < 50 ppb). Vacuum towers usually are not able to reach such a low content and have to be coupled with an oxygen scavenger [10]. At the same time, the seawater pH (around 8) must often be decreased for the pre-treatment steps (for example, a neutral value is needed when coagulation is used as pre-treatment), and H<sub>2</sub>SO<sub>4</sub> is typically employed.

If gas-liquid MCs are applied, it is possible to couple the oxygen removal with the pH reduction in the same device, by sending carbon dioxide in the gas phase. Figure 7 shows the maximum variations registered in [23] for seawater.

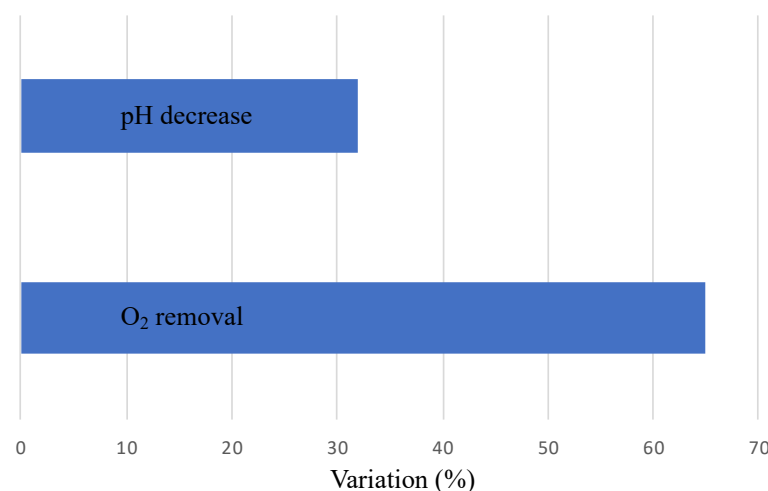


Figure 7. Maximum variations registered in [23] for the seawater pre-treatment.

A maximum pH reduction of 32% was obtained for seawater (from 7.83 to 5.32). Therefore, gas-liquid MCs can be used to decrease the seawater pH down to 7, as required,

by simply acting on the operating time. Concerning the oxygen removal, a maximum of 65% oxygen removal was obtained, while higher values (around 99.7%) are needed to meet the specification. As reported in Section 2.1.2., the transport of gaseous species in the membrane contactor mainly depends on the mass transfer coefficients of the liquid and of the membrane. This means that variations at the gas side (e.g., an increase of the gas flow rate) would lead to improvement of the removal efficiency less than acting on the liquid side or on the membrane properties would. By applying the equations reported in Section 2.1.2, both mass transfer coefficients were calculated, to theoretically analyze the obtained result. In particular, for the membrane used in [23], which gave the values reported in Figure 7, only the membrane pore size (nominal diameter of 0.2 μm) and the thickness (202 μm) were known. Therefore, calculations were made by varying the porosity of the membrane from 20% to 80% and by using both formulae available to obtain the tortuosity. Figure 8 shows the trend of the mass transfer coefficient of the membrane over the porosity. In both cases, an increase of the membrane porosity leads to an increase of  $k_m$ , because of the higher area available for the transport. This is more evident for the case of a more open structure of the membrane. However, the mass-transfer coefficient of the membrane is always much higher than that of the liquid phase, as shown in Figure 9, where the lowest  $k_m$  values are compared with the calculated  $k_l$ .

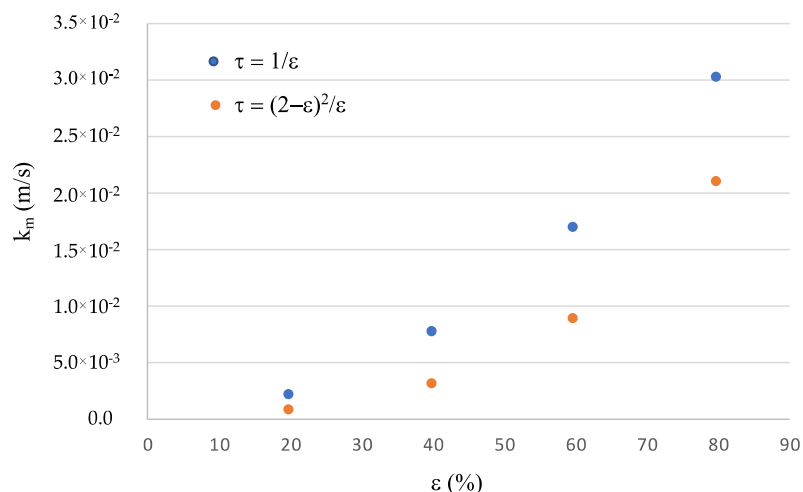


Figure 8. Mass transfer coefficient of the membrane as function of the membrane porosity and structure.

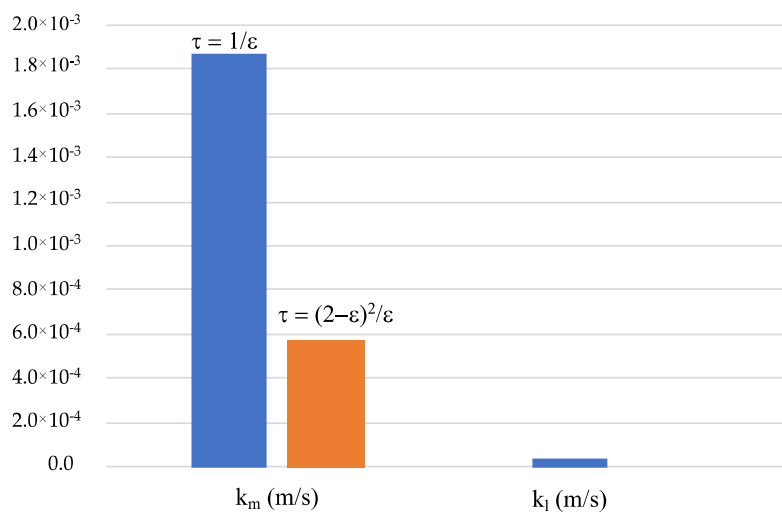


Figure 9. Comparison of the mass transfer coefficients.

This means that, to achieve the target of the oxygen removal with membrane contactors, it is necessary to reduce the mass-transfer resistance of the liquid side. This is possible by changing the module design and/or increasing the liquid-flow rate. As previously noted, the experimental liquid flow rate was the maximum for the lab setup used, and no further increase can be made. Moreover, the membrane module used for the lab tests was characterized by a parallel flow of the liquid on the membrane surface, and no baffles or turbulence promoters were present. Therefore, with the used system, the target for oxygen removal cannot be reached and changes/improvements to the module design are required. Nevertheless, removals of 99.83% were achieved with commercial membrane contactors [24], confirming the efficiency of the process. The commercial membrane module was, in fact, characterized by the presence of a central baffle which forced the liquid to flow perpendicularly to the membrane surface, leading to a reduction of the mass transport resistances at the liquid side. In this case, hollow-fiber membranes were used. Once the module design is defined, the oxygen-removal target and the desired pH can be obtained in the same unit by properly acting on the operating conditions. For instance, if the final pH is lower than 7, due to the improved mass transfer coefficient at the liquid side, the target value can be obtained by supplying CO<sub>2</sub> mixed with N<sub>2</sub> (in appropriate amounts) or by combining CO<sub>2</sub> with a vacuum.

### 3.1.2. Case Study 2: The Post-Treatment of the RO Permeate to Increase the pH

After the RO permeate remineralization, its pH has to be increased (typically between 7.5 and 8.5), and NaOH addition or CO<sub>2</sub> stripping are commonly used [1]. To avoid the use of NaOH, and to work with a more compact system than a stripping tower, stripping with nitrogen in the gas-liquid MC can be adopted. Based on the results of [23], a pH increase of 30% was reached for the RO permeate (from 5.83 to 7.58). Therefore, MCs can be used to match the target for product water.

## 3.2. RO Brine Treatment

Figure 10a shows the effects of the feed concentration and temperature on the flux achievable in DCMD. The flux was strongly influenced by the operating temperature, due to the exponential increase in the vapor pressure at the feed side, which translates to a higher driving force across the membrane. As expected, the flux was only slightly affected by the amount of salt in the feed, and it decreased moving from seawater to RO brine by 6% and 9% at 40 °C and 80 °C, respectively. The higher flux reduction registered at 80 °C can be attributed to the higher permeate flux and to the consequent higher increase of the feed concentration, which reduces the vapor pressure. When comparing the permeate conductivity, no big differences were noticed. The highest difference was registered for the tests carried out on the RO brine (see Figure 10b). In this case, the conductivity was 2.3 μS/cm ( $2.3 \times 10^{-4}$  S/m) and 2.8 μS/cm ( $2.8 \times 10^{-4}$  S/m) for 40 °C and 80 °C, respectively. This result can be due to the higher permeate flux that, at higher feed concentrations, might entrain some more salt from the feed to the permeate side. Nevertheless, the permeate conductivity was still very low, with rejection values > 99.99%.

By comparing the results obtained at the two temperatures for the 80 g/L feed, the increase of flux registered at 80 °C was significantly higher than the related increase of the permeate conductivity. This means that a higher amount of fresh water can be obtained. However, higher temperatures also imply higher thermal energy demand, and a trade-off must be reached. When waste heat or renewable energies (e.g., solar) are available and appropriate pre-treatments are conceived, the use of high temperatures in DCMD allows increase in the productivity of the process and, then, of the RO desalination plant.

The behavior of the flux with time is reported in Figure 11. In the first 30 min of operation, a slight decline in flux was registered, then, in the remaining time of the test, the flux was quite stable.

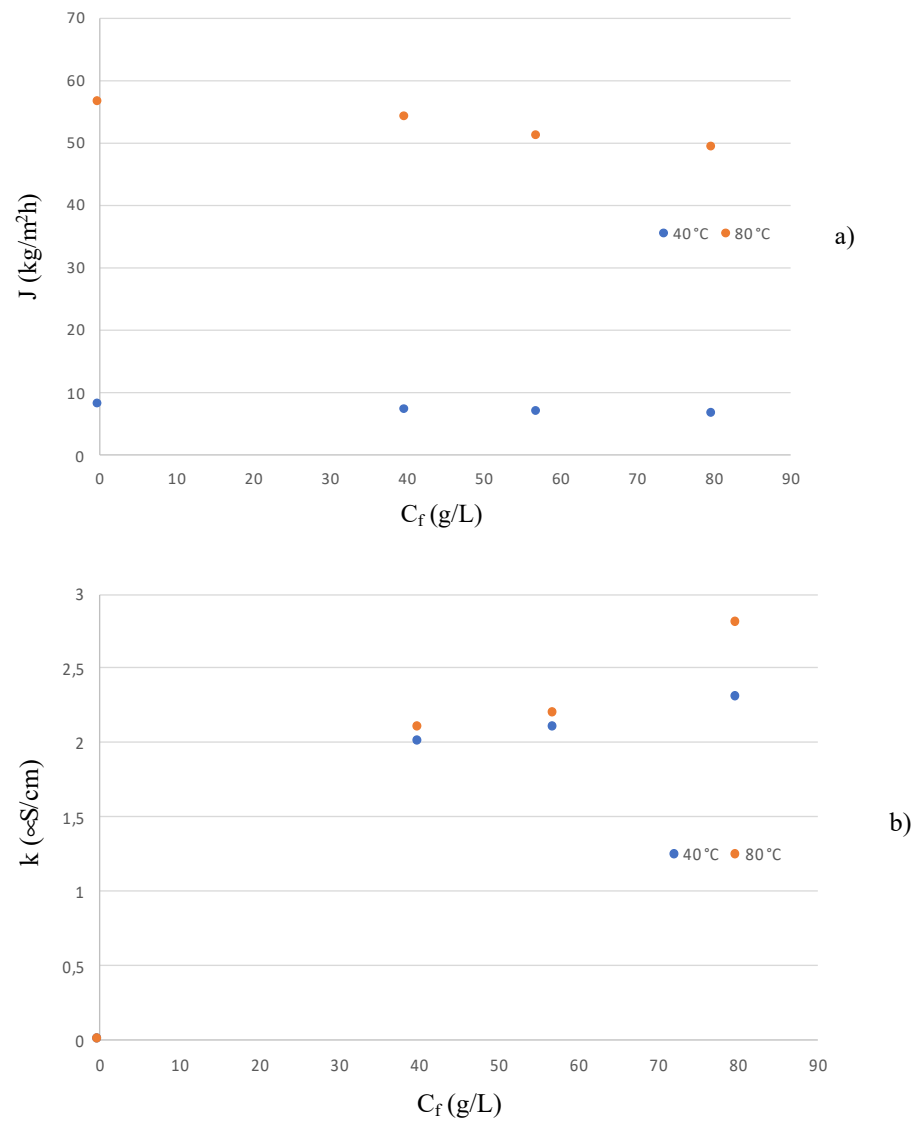


**Figure 10.** DCMD tests. Effect of feed temperature and concentration on (a) the flux and (b) the permeate conductivity.

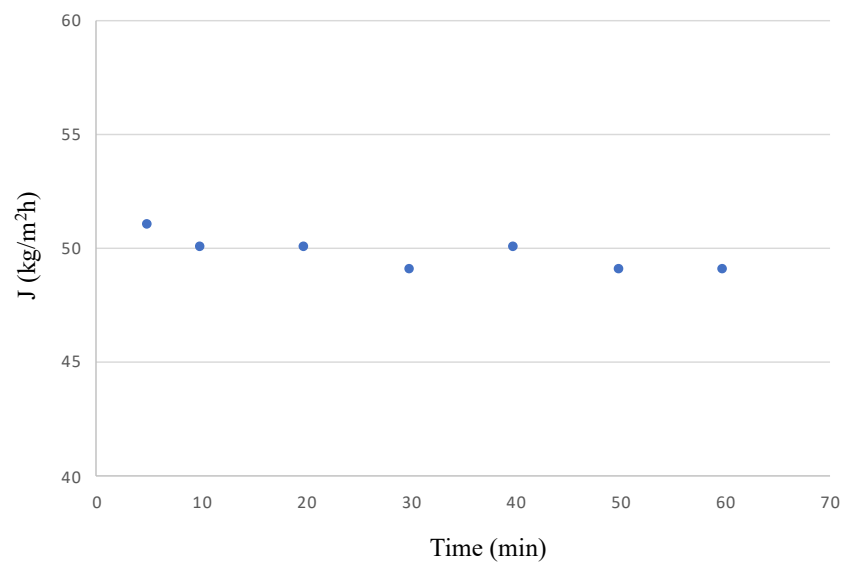


**Figure 11.** DCMD tests. The trend of the flux with time. Feed: 80 g/L; 80 °C.

Similar tests were performed with the VMD configuration. Figure 12 summarizes the trend of the flux at 40 °C and 60 °C and as a function of the feed concentration. Also in this case, there was a reduction of flux with the increase of the feed concentration, and higher fluxes were obtained at higher temperatures due to the higher driving forces. Yet interesting flux values were already obtained at 40 °C. In fact, if we compare the DCMD and VMD configuration at parity of feed temperature, a significant difference in flux is registered, despite applying the same driving force (Figure 13). The two MD configurations operate in the same conditions at the feed side, so this difference in performance can be linked to different conditions established at the permeate side. In particular, while 20 mbar was the effective pressure at the permeate side in VMD, the vapor pressure at the membrane-distillate side can be higher than that of the bulk, due to temperature polarization, with a consequent decrease of the effective driving force in DCMD.

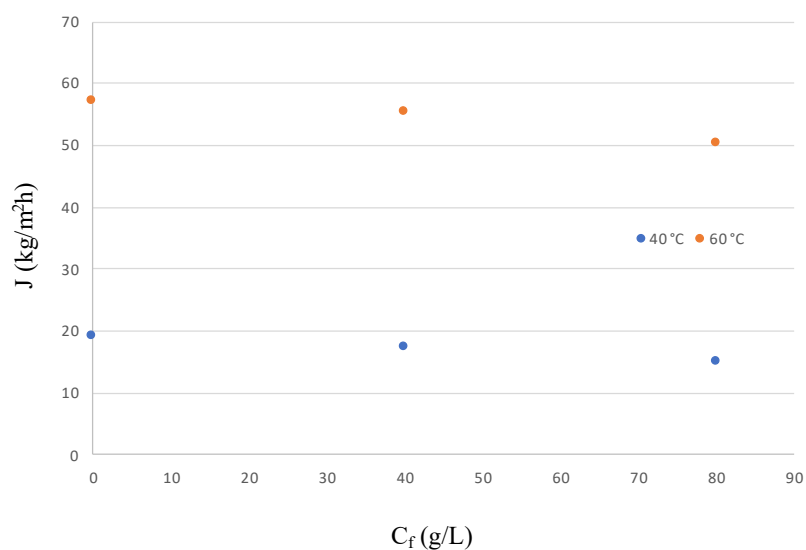


Figure 12. VMD tests. Effect of feed temperature and concentration on the flux.

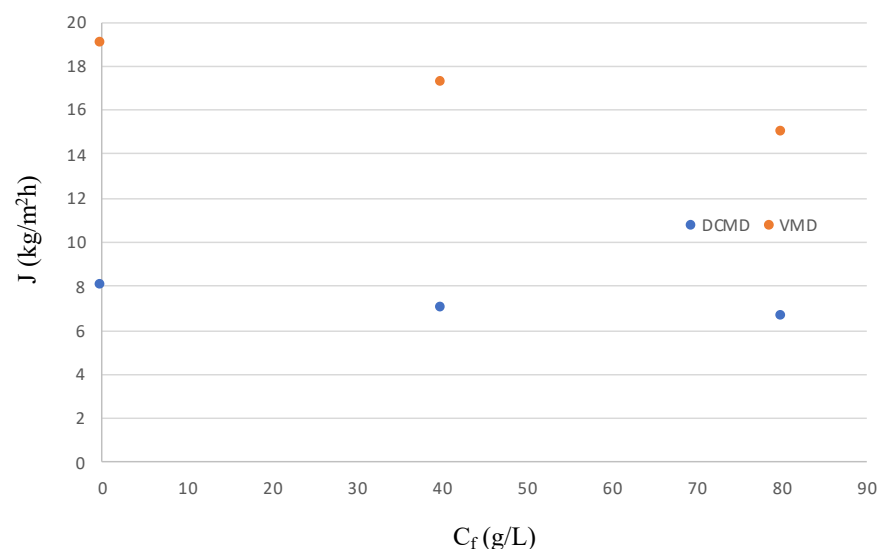


Figure 13. Comparison of DCMD and VMD at 40 °C.

The higher driving force of the VMD configuration allowed the same DCMD fluxes to be obtained at a lower feed temperature (60 °C vs. 80 °C), without affecting the permeate quality (see Table 2), with a consequent reduction of the thermal energy consumption.

However, VMD is more prone to wetting than DCMD, and long-term experiments are needed to better evaluate this aspect.

**Table 2.** Comparison of DCMD and VMD operating on the 80 g/L brine.

MD Configuration	Flux (kg/m <sup>2</sup> h)	Permeate Conductivity (μS/cm)
DCMD (80 °C)	49	2.8
VMD (60 °C)	50.3	3.0

Table 3 summarizes main data available in the literature (2009–2022) for the treatment of RO brines by membrane distillation. In particular, the initial flux is reported, so as to make a comparison with the results obtained in this work. As can be seen, DCMD was the most-investigated configuration, followed by Air Gap Membrane Distillation (AGMD). A flat geometry of the membrane module was considered, with membrane areas ranging from 9.1 cm<sup>2</sup> up to 8.34 m<sup>2</sup>. Membranes used were also different, as were the feed concentrations and temperatures. All these factors led to a significant variation of the achievable flux. For instance, the highest flux has been obtained for DCMD working with the thinnest membrane, which also had the biggest pore size. The lowest flux values have been registered for the AGMD configuration, due to the higher mass-transfer resistance offered by the air gap present in the module. Interestingly, when comparing DCMD and VMD, in most cases DCMD gave higher fluxes, in contrast with the typical feature of VMD, which is known as the MD configuration leading to the highest fluxes. This result is due to the large number of conditions varied in the literature studies, which makes impossible a direct comparison of the performances. In this work, by operating in the same conditions, VMD led to higher fluxes than DCMD. The better performance of VMD has also been reported in other literature studies, where the two MD configurations have been compared at the same feed temperature and concentration [28–36]. This confirms the aim of the present study, where exactly the same operating conditions, module, membrane and applied driving force were used to compare DCMD and VMD for the treatment of the RO brine. It has to finally be noted that, considering the different conditions used, the experimental fluxes obtained in this work are in agreement with what is reported in the literature (see Table 3).

**Table 3.** Main literature data for the treatment of RO brines by MD.

MD Configuration	Module (Area)	Membrane (d <sub>p</sub> ; ε, δ)	Feed (g/L)	Flux (kg/m <sup>2</sup> h)	Ref.
VMD (55 °C)	Flat (9.1 cm <sup>2</sup> )	0.2 μm; 75%; 163 μm	100	14.4	[12]
VMD (50 °C)	Flat (57.8 cm <sup>2</sup> )	0.22 μm; 40%; 175 μm	64	17	[13]
AGMD (62 °C)	Flat (2.8 m <sup>2</sup> )	0.05–0.2 μm; n.a.; n.a.	39.5	2	[14]
AGMD (50 °C)	Flat (143.5 cm <sup>2</sup> )	0.2 μm; n.a.; 175 μm	80	0.15	[15]
DCMD (50 °C)	Flat (14.4 cm <sup>2</sup> )	0.22 μm; 82%; 35 μm	88	17	[16]
DCMD (75 °C)	Flat (39.4 cm <sup>2</sup> )	0.33 μm; 78%; 107 μm	55	52.3	[17]
DCMD (70 °C)	Flat (25 cm <sup>2</sup> )	0.45 μm; 73%; 113 μm	49.6	72.3	[18]
AGMD (80 °C)	Spiral wound (8.34 m <sup>2</sup> )	0.2 μm; 80%; 76 μm	80	1.5	[20]

Table 3. Cont.

MD Configuration	Module (Area)	Membrane ( $d_p$ ; $\epsilon$ , $\delta$ )	Feed (g/L)	Flux (kg/m <sup>2</sup> h)	Ref.
DCMD (50 °C)	Flat (n.a.)	n.a.; 88.6%; 115 $\mu$ m	292	8	[21]
DCMD (70 °C)	Flat (100 cm <sup>2</sup> )	0.3–0.7 $\mu$ m; n.a.; 15.5 $\mu$ m	75.5	120	[22]
DCMD (73 °C)	Flat (26.4 cm <sup>2</sup> )	0.49 $\mu$ m; 78%; 82 $\mu$ m	70	16	[29]
DCMD (80 °C)	Flat (40 cm <sup>2</sup> )	0.2 $\mu$ m; 70%; 91 $\mu$ m	80	49	This work
VMD (60 °C)	Flat (40 cm <sup>2</sup> )	0.2 $\mu$ m; 70%; 91 $\mu$ m	80	50.3	This work

$p$ : mean pore diameter.

#### 4. Conclusions

Membrane contactors can find interesting applications in desalination plants. Their features make them attractive for both gas-liquid operations and membrane distillation. The ability to cover different processes is an indication of MCs' flexibility, which is an important aspect in the plant design. Moreover, the possibility of using the same module for the different applications positively impacts the simplification and economy of the project. When used for the pH control, a maximum pH reduction of 32% is obtained for seawater (from 7.83 to 5.32), with the possibility of reaching the target of neutral pH, needed when coagulation is used in the RO pre-treatment, by simply acting on the operating time. A pH increase of 30% is reached for the RO permeate (from 5.83 to 7.58), matching the target for product water. The maximum oxygen removal of 65% obtained with the lab set-up can be increased up to the desired target by acting on the module design, so as to reduce the mass transfer resistance at the liquid side. MCs are, therefore, able to avoid/reduce the use of chemicals in the RO plant, also resulting in plants being more compact than traditional vacuum/stripping towers. By using the same module, membrane, and operating conditions for the RO brine treatment, it is possible to make a direct comparison of DCMD and VMD configuration performances. Both configurations are able to produce fresh water from the 80 g/L RO brine, thus increasing the overall water recovery factor while reducing the RO brine volume. At the same applied driving force (DCMD: 40 °C–18 °C; VMD: 40 °C–20 mbar), the DCMD configuration leads to a lower flux than the VMD one (6.6 kg/m<sup>2</sup>h vs. 15 kg/m<sup>2</sup>h) because of the temperature polarization at the permeate side. Similar fluxes and permeate conductivities are obtained when working at 60 °C in VMD and at 80 °C in DCMD. Despite the better performance of VMD, the higher risk of membrane wetting needs to be carefully evaluated. Finally, both configurations lead to salt rejections > 99.99%, confirming the production of high-quality permeates. Membrane contactors represent, therefore, interesting and flexible membrane operations to be applied for improving the efficiency and reducing the environmental impact of desalination plants.

**Supplementary Materials:** The following supporting information can be downloaded at: <https://www.mdpi.com/article/10.3390/separations10020129/s1>, Figure S1: Gas-Liquid set-up.; Figure S2: DCMD set-up.; Figure S3: VMD set-up.

**Funding:** This research received no external funding.

**Data Availability Statement:** The data presented in this study are available within the article.

**Conflicts of Interest:** The author declares no conflict of interest.

## References

1. Voutchkov, N. Re-Mineralization of Desalinated Water. Available online: [www.SunCam.com](http://www.SunCam.com) (accessed on 9 December 2022).
2. Roberts, D.A.; Johnston, E.L.; Knott, N.A. Impacts of desalination plant discharges on the marine environment: A critical review of published studies. *Water Res.* **2010**, *44*, 5117–5128. [[CrossRef](#)] [[PubMed](#)]
3. van der Merwe, R.; Bleninger, T.; Scedo-Feliz, D.; Lattemann, S.; Amy, G. Combining autonomous underwater vehicle missions with velocity and salinity measurements for the evaluation of a submerged offshore SWRO concentrate discharge. *J. Appl. Water Eng. Res.* **2014**, *2*, 118–139. [[CrossRef](#)]
4. Heck, N.; Lykkebo Petersen, K.; Potts, D.C.; Haddad, B.; Paytan, A. Predictors of coastal stakeholders' knowledge about seawater desalination impacts on marine ecosystems. *Sci. Total Environ.* **2018**, *639*, 785–792. [[CrossRef](#)] [[PubMed](#)]
5. Petersen, K.L.; Paytan, A.; Rahav, E.; Levy, O.; Silverman, J.; Barzel, O.; Bar-Zeev, E. Impact of brine and antiscalants on reef-building corals in the Gulf of Aqaba—Potential effects from desalination plants. *Water Res.* **2018**, *144*, 183–191. [[CrossRef](#)] [[PubMed](#)]
6. Gabelman, A.; Hwang, S.-T. Hollow fiber membrane contactors. *J. Membr. Sci.* **1999**, *158*, 61–106. [[CrossRef](#)]
7. Drioli, E.; Criscuoli, A.; Curcio, E. *Membrane Contactors: Fundamentals, Applications and Potentialities*, 1st ed.; Elsevier: Amsterdam, The Netherlands, 2006; pp. 1–502.
8. 3MTM Liqui-Cel™ Membrane Contactor Technology Being Evaluated for Dissolved Gas Removal from Water in Many Hydrocarbon Processes. Available online: <https://multimedia.3m.com/mws/media/14126290/technology-evaluated-dissolved-gas-removal-hydrocarbon-proc.pdf> (accessed on 9 December 2022).
9. Degassing Sea Water Has Never Been This Compact, Efficient, and Adaptable. Available online: <https://multimedia.3m.com/mws/media/14126270/3m-liqui-cel-membrane-contactors-degassing-sea-water.pdf> (accessed on 9 December 2022).
10. Oxygen Removal from Injection Seawater in Offshore Platforms: Vacuum Tower Versus Membrane Deaeration Technology. Available online: [www.cannonartes.com](http://www.cannonartes.com) (accessed on 9 December 2022).
11. Qu, D.; Wang, J.; Fan, B.; Luan, Z.; Hou, D. Study on concentrating primary reverse osmosis retentate by direct contact membrane distillation. *Desalination* **2009**, *247*, 540–550. [[CrossRef](#)]
12. Safavi, M.; Mohammadi, T. High-salinity water desalination using VMD. *Chem. Eng. J.* **2009**, *149*, 191–195. [[CrossRef](#)]
13. Mericq, J.P.; Laborie, S.; Cabassud, C. Vacuum membrane distillation of seawater reverse osmosis brines. *Water Res.* **2010**, *44*, 5260–5273. [[CrossRef](#)]
14. Basha, K.S.A.; Dolfe, H.; Aslin, M.; El-Gabry, L. Membrane Distillation Test for Concentration of RO Brine at WESSCO, Jeddah. In Proceedings of the IDA World Congress, Perth, WA, Australia, 4–9 September 2011.
15. Alkhudhiri, A.; Darwish, N.; Hilal, N. Treatment of high salinity solutions: Application of air gap membrane distillation. *Desalination* **2012**, *287*, 55–60. [[CrossRef](#)]
16. Guan, Y.; Li, J.; Chen, F.; Zhao, J.; Wang, X. Influence of salt concentration on DCMD performance for treatment of highly concentrated NaCl, KCl, MgCl<sub>2</sub> and MgSO<sub>4</sub> solutions. *Desalination* **2015**, *355*, 110–117. [[CrossRef](#)]
17. Sanmartino, J.A.; Khayet, M.; Garcia-Payo, M.C.; El-Bakouri, H.; Riaza, A. Treatment of reverse osmosis brine by direct contact membrane distillation: Chemical pretreatment approach. *Desalination* **2017**, *420*, 79–90. [[CrossRef](#)]
18. Yan, Z.; Yang, H.; Qu, F.; Yu, H.; Liang, H.; Li, G.; Ma, J. Reverse osmosis brine treatment using direct contact membrane distillation: Effects of feed temperature and velocity. *Desalination* **2017**, *423*, 149–156. [[CrossRef](#)]
19. Yan, Z.; Yang, H.; Yu, H.; Qu, F.; Liang, H.; Van der Bruggen, B.; Li, G. Reverse osmosis brine treatment using direct contact membrane distillation (DCMD): Effect of membrane characteristics on desalination performance and the wetting phenomenon. *Environ. Sci. Water Res. Technol.* **2018**, *4*, 428–437. [[CrossRef](#)]
20. Schwantes, R.; Bauer, L.; Chavan, K.; Ducher, D.; Felsmann, C.; Pfafferott, J. Air gap membrane distillation for hypersaline brine concentration: Operational analysis of a full-scale module—New strategies for wetting mitigation. *Desalination* **2018**, *444*, 13–25. [[CrossRef](#)]
21. Al-Furaihi, M.; Arena, J.T.; Ren, J.; Benes, N.; Nijmeijer, A.; McCutcheon, J.R. Triple-layer nanofiber membranes for treating high salinity brines using direct contact membrane distillation. *Membranes* **2019**, *9*, 60. [[CrossRef](#)]
22. Abdelrazeq, H.; Khraisheh, M.; Hassan, M.K. Long-term treatment of highly saline brine in a direct contact membrane distillation (DCMD) pilot unit using polyethylene membranes. *Membranes* **2022**, *12*, 424. [[CrossRef](#)]
23. Criscuoli, A.; Carnevale, M.C.; Mahmoudi, H.; Gaeta, S.; Lentini, F.; Drioli, E. Membrane contactors for the oxygen and pH control in desalination. *J. Membr. Sci.* **2011**, *376*, 207–213. [[CrossRef](#)]
24. Criscuoli, A.; Drioli, E.; Moretti, U. Membrane contactors in beverage industry for controlling the water gas composition. *Ann. N. Y. Acad. Sci.* **2003**, *984*, 1–16. [[CrossRef](#)]
25. Lawson, K.W.; Lloyd, D.R. Membrane distillation. *J. Membr. Sci.* **1997**, *124*, 1–25. [[CrossRef](#)]
26. Hashemifard, S.A.; Ismail, A.F.; Matsuura, T.; Rezaei DashtArzhandi, M. Performance of silicon rubber coated polyetherimide hollow fibers for CO<sub>2</sub> removal via a membrane contactor. *RSC Adv.* **2015**, *5*, 48442–48455. [[CrossRef](#)]
27. Iversen, S.B.; Bhatia, V.K.; Dam-Johansen, K.; Jonsson, G. Characterization of microporous membranes for use in membrane contactors. *J. Membr. Sci.* **1997**, *130*, 205–217. [[CrossRef](#)]
28. Tang, Y.; Li, N.; Liu, A.; Ding, S.; Yi, C.; Liu, H. Effect of spinning conditions on the structure and performance of hydrophobic PVDF hollow fiber membranes for membrane distillation. *Desalination* **2012**, *287*, 326–339. [[CrossRef](#)]

29. Fan, H.; Peng, Y. Application of PVDF membranes in desalination and comparison of the VMD and DCMD processes. *Chem. Eng. Sci.* **2012**, *79*, 94–102. [[CrossRef](#)]
30. Drioli, E.; Ali, A.; Simone, S.; Macedonio, F.; AL-Jilil, S.A.; Al Shabonah, F.S.; Al-Romaih, H.S.; Al-Harbi, O.; Figoli, A.; Criscuoli, A. Novel PVDF hollow fiber membranes for vacuum and direct contact membrane distillation applications. *Sep. Pur. Technol.* **2013**, *115*, 27–38. [[CrossRef](#)]
31. Zhang, J.W.; Fang, H.; Wang, J.W.; Hao, L.Y.; Xu, X.; Chen, C.S. Preparation and characterization of silicon nitride hollow fiber membranes for seawater desalination. *J. Membr. Sci.* **2014**, *450*, 197–206. [[CrossRef](#)]
32. Carnevale, M.C.; Gnisci, E.; Hilal, J.; Criscuoli, A. Direct Contact and Vacuum Membrane Distillation application for the olive mill wastewater treatment. *Sep. Purif. Technol.* **2016**, *169*, 121–127. [[CrossRef](#)]
33. Ramlow, H.; Machado, R.A.F.; Bierhalz, A.C.K.; Marangoni, C. Influence of dye class on the comparison of direct contact and vacuum membrane distillation applied to remediation of dyeing wastewater. *J. Environ. Sci. Health Part A* **2019**, *54*, 1337–1347. [[CrossRef](#)]
34. Schnittger, J.; McCutcheon, J.; Hoyer, T.; Weyd, M.; Fischer, G.; Puhlfürß, P.; Halisch, M.; Voigt, I.; Lerch, A. Hydrophobic ceramic membranes in MD processes—Impact of material selection and layer characteristics. *J. Membr. Sci.* **2021**, *618*, 118678. [[CrossRef](#)]
35. Sparenberg, M.-C.; Hanot, B.; Molina-Fernández, C.; Luis, P. Experimental mass transfer comparison between vacuum and direct contact membrane distillation for the concentration of carbonate solutions. *Sep. Pur. Technol.* **2021**, *275*, 119193. [[CrossRef](#)]
36. Guan, G.; Yang, X.; Wang, R.; Field, R.; Fane, A.G. Evaluation of hollow fiber-based direct contact and vacuum membrane distillation systems using aspen process simulation. *J. Membr. Sci.* **2014**, *464*, 127–139. [[CrossRef](#)]

**Disclaimer/Publisher’s Note:** The statements, opinions and data contained in all publications are solely those of the individual author(s) and contributor(s) and not of MDPI and/or the editor(s). MDPI and/or the editor(s) disclaim responsibility for any injury to people or property resulting from any ideas, methods, instructions or products referred to in the content.